Circular and elliptical birefringence in spun microstructured optical fibres

Alexander Argyros[1], Jarryd Pla[1,2], François Ladouceur[2], Leon Poladian[3]

[1]*Institute of Photonics and Optical Science (IPOS), School of Physics, The University of Sydney, NSW 2006, Australia*

[2] *School of Electrical Engineering and Telecommunications, University of New South Wales, NSW 2052, Australia*

[3]*School of Mathematics and Statistics, The University of Sydney, NSW 2006, Australia*

a.argyros@usyd.edu.au

Abstract: We investigate circular birefringence induced by spinning microstructured optical fibres during their fabrication to produce helical-shaped holes. Designs with an offset core which results in a helical path for the light and exhibit only circular birefringence and designs with a linearly birefringent core that result in elliptical birefringence are both investigated.

OCIS codes: (060.2310) Fiber optics; (060.2300) Fiber measurements; (060.2400) Fiber properties; (060.5295) Photonic crystal fibers; (260.5430) Polarization

References and links

1. J. Noda, K. Okamoto, and Y. Sasaki, "Polarization-maintaining fibers and their applications," J. Lightwave Technol. **4**(8), 1071–1089 (1986).
2. P. St. J. Russell, "Photonic-cystal fibers," J. Lightwave Technol. **24**(12), 4729–4749 (2006).
3. M. C. J. Large, L. Poladian, G. W. Barton, and M. A. van Eijkelenborg, *Microstructured polymer optical fibres* (Springer, Berlin, 2007).
4. A. Argyros, "Microstructured polymer optical fibres," J. Lightwave Technol. **27**(11), 1571–1579 (2009).
5. N. A. Issa, M. A. van Eijkelenborg, M. Fellew, F. Cox, G. Henry, and M. C. J. Large, "Fabrication and study of microstructured optical fibers with elliptical holes," Opt. Lett. **29**(12), 1336–1338 (2004).
6. H. Kubota, S. Kawanishi, S. Koyanagi, M. Tanaka, and S. Yamaguchi, "Absolutely single polarization photolnic crystal fiber," IEEE Photon. Technol. Lett. **16**(1), 182–184 (2004).
7. J. N. Ross, "The rotation of the polarization in low birefringence monomode optical fibres due to geometric effects," Opt. Quantum Electron. **16**(5), 455–461 (1984).
8. M. P. Varnham, R. D. Birch, and D. N. Payne, "Helical-core circularly birefringent fibres," In Proc. IOOC-ECOC, Venice, 1985.
9. J. Qian, "Coupled-mode theory for helical fibres," IEE Proceedings J. **135**, 178–182 (1988).
10. R. D. Birch, "Fabrication and characterisation of circularly birefringent helical fibres," Electron. Lett. **23**(1), 50–52 (1987).
11. A. Altintas, and J. D. Love, "Effective cut-offs for modes on helical fibres," Opt. Quantum Electron. **22**(3), 213–226 (1990).
12. R. I. Laming, and D. N. Payne, "Electric current sensors employing spun highly birefringent optical fibers," J. Lightwave Technol. **7**(12), 2084–2094 (1989).
13. J. R. Qian, Q. Guo, and L. Li, "Spun linear birefringence fibres and their sensing mechanism in current sensors with temperature compensation," IEE Proceedings J. **141**, 373–380 (1994).
14. A. Michie, J. Canning, I. Bassett, J. Haywood, K. Digweed, M. Åslund, B. Ashton, M. Stevenson, J. Digweed, A. Lau, and D. Scandurra, "Spun elliptically birefringent photonic crystal fibre," Opt. Express **15**(4), 1811–1816 (2007), http://www.opticsinfobase.org/oe/abstract.cfm?URI=oe-15-4-1811.
15. E. Udd, *Fiber optic sensors* (John Wiley & Sons, Inc., New York, 1991).
16. V. P. Gubin, V. A. Isaev, S. K. Morshnev, A. I. Sazonov, N. I. Starostin, Y. K. Chamorovsky, and A. I. Oussov, "Use of spun optical fibres in current sensors," Quantum Electron. **36**(3), 287–291 (2006).
17. M. Fuochi, J. Hayes, K. Furusawa, W. Belardi, J. Baggett, T. Monro, and D. Richardson, "Polarization mode dispersion reduction in spun large mode area silica holey fibres," Opt. Express **12**(9), 1972–1977 (2004), http://www.opticsinfobase.org/oe/abstract.cfm?URI=oe-12-9-1972.
18. P. Wang, L. J. Cooper, J. K. Sahu, and W. A. Clarkson, "Efficient single-mode operation of a cladding-pumped ytterbium-doped helical-core fiber laser," Opt. Lett. **31**(2), 226–228 (2006).
19. C. N. Alexeyev, and M. A. Yavorsky, "Optical vortices and the higher order modes of twisted strongly elliptical optical fibres," J. Opt. A, Pure Appl. Opt. **6**(9), 824–832 (2004).
20. J. Qian, and C. D. Hussey, "Circular birefringence in helical-core fibre," Electron. Lett. **22**(10), 515–517 (1986).
21. R. Ulrich, and A. Simon, "Polarization optics of twisted single-mode fibres," Appl. Opt. **18**(13), 2241–2251 (1979).

#113937 - $15.00 USD Received 13 Jul 2009; revised 19 Aug 2009; accepted 19 Aug 2009; published 25 Aug 2009

22. T. A. Birks, J. C. Knight, and P. St. J. Russell, "Endlessly single-mode photonic crystal fiber," Opt. Lett. **22**(13), 961–963 (1997).

1. Introduction

Birefringence in optical fibres has been utilised to achieve some control over the polarisation state of the light propagating along the fibre. Linear birefringence is induced through 2-fold symmetric asymmetries in the fibre cross section [1]. These may be in the form of an elliptical core, or, in the context of microstructured optical fibres [2–4], asymmetries in the hole pattern such as oriented elliptical holes [5] or two larger holes on opposite sides of the core [6]. Circular birefringence may be produced through a break in the longitudinal symmetry of the waveguide, which can be achieved by spinning the fibre to produce a helical structure. If the core of the fibre is placed off-centre, spinning will result in a helical-core fibre [7–11]. If the core is centred in the fibre, then an asymmetry in the cross-section is required to produce the longitudinal asymmetry, meaning the fibre must be linearly birefringent to begin with – a spun linearly-birefringent (SLB) fibre [12–14]. Helical core fibres will be circularly birefringent in the absence of any linear birefringence, whilst in SLB fibres the linear and circular components will combine to produce elliptical birefringence.

Any birefringence breaks the degeneracy of the fundamental mode to produce two separate orthogonally polarised modes that travel with different phase velocities in the fibre. Linear birefringence results in these two modes having linear polarisation oriented along the two symmetry axes of the fibre. Circular birefringence produces right- and left-hand circularly polarised modes whilst elliptical birefringence results in two elliptically polarised modes with their major axes oriented along the symmetry axes of the fibre. The birefringence B is the difference in the mode effective indices n_{eff} of the two polarisation modes; $B = n_{\text{eff},1} - n_{\text{eff},2}$.

If light is launched into one of these polarisation modes, this difference in effective index will reduce coupling to the other polarisation state, and the polarisation of the light will be preserved. If light is launched into both, the polarisation state will evolve along the fibre as the phase difference between the two polarisation modes (travelling at different phase velocities) accumulates. The length of fibre required to bring the two polarisation modes back in phase and reproduce the original polarisation state is the beat length L_B,

$$L_B = \lambda / B. \tag{1}$$

The evolution of the polarisation state can be represented on the Poincare Sphere shown in Fig. 1 [15]. The two polarisation modes have orthogonal polarisations and so are placed at opposite points on the Sphere. An arbitrary input polarisation will rotate on the Poincare Sphere about the birefringence axis defined by the two polarisation modes, so as to trace a circle as in Fig. 1. The polarisation of the light will process around this circle as it propagates along the fibre. At a particular position along the fibre, the light of different wavelengths may be spread around the circle depending on the wavelength dependence of the birefringence.

Both helical-core and SLB fibres have been reported in the literature, e.g [10, 12]. The highest circular birefringence reported in a helical-core fibre was 2.11×10^{-4}, giving a beat length of 3 mm at 633 nm [10]. This fibre had a core offset of 340 μm and a pitch of 2 mm. SLB fibres have also been reported with the most relevant example to this work being a spun birefringent silica microstructured fibre with an elliptical birefringence of 1.8×10^{-3}, giving a beat length of 0.88 mm at 1550 nm [14]. The pitch was 7.7 mm and the ellipticity was 0.115 (the linear birefringence dominated). The interest in spun fibres arises from applications in current sensing [12,13,16], where inducing sufficient circular birefringence into the fibre to swamp the intrinsic and extrinsic sources of linear birefringence is an important requirement for measuring Faraday rotation, as well as in producing low birefringence for the reduction of polarisation mode dispersion [17]. Circularly birefringent fibres have also been investigated for eliminating higher order modes in large-mode-area fibre lasers [18] and in the study of optical vortices [19]. In this paper we aim to investigate the effects of spinning

#113937 - $15.00 USD Received 13 Jul 2009; revised 19 Aug 2009; accepted 19 Aug 2009; published 25 Aug 2009

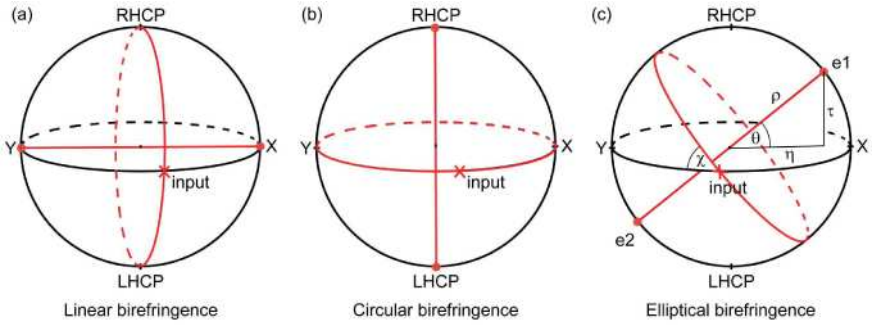

Fig. 1. The Poincare Sphere representation of polarisation, in which the poles represent right-hand and left-hand circular polarisation (RHCP, LHCP) and the equator linear polarisation. The polarisation modes are denoted by red circles and the polarisation axis is shown for (a) linear, (b) circular and (c) elliptical birefringence. Light that excites both polarisation modes (figure assumes these are equally excited) will trace out a circle as shown as it propagates along the fibre.

microstructured polymer optical fibres (mPOF) [3,4] to assess the range of circular birefringence that can be practically achieved in these fibres. Both helical-core and SLB fibres are investigated.

2. Fibre fabrication

The fibres used in this work were drawn from 8 cm diameter polymethylmethacrylate (PMMA) preforms into which the appropriate pattern of holes had been drilled. The preforms were stretched to 10 mm diameter intermediate preforms from which the fibres were drawn [3,4]. In one case, the hole pattern was drilled off centre so as to produce a helical core, whilst in the other the hole pattern was centred and pressure was selectively applied to two holes adjacent to the core so as to produce the required linear birefringence.

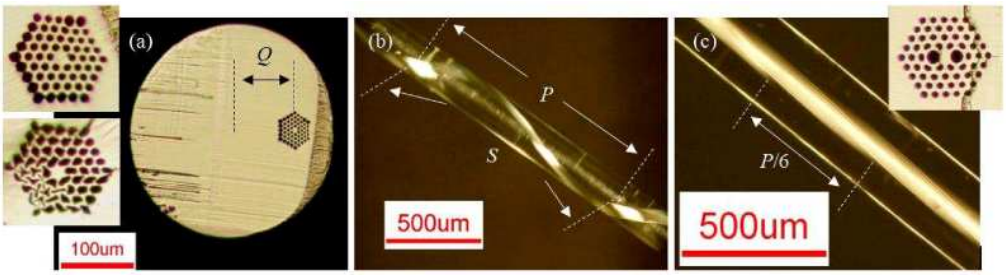

Fig. 2. (a) Cross-section of a helical-core fibre. The insets compare the distortion to the microstructure created by spinning (upper inset - 13 mm pitch, compared to lower inset - 1.88 mm pitch). (b) Side-view of helical fibre. (c) Side view of SLB fibre with inset showing the cross section. The spin pitch P, the core off-set Q and the arc length of the helix S are indicated.

The fibres were drawn at temperature of 180 – 200 °C and were spun at rates of up to 500 RPM. A rotary seal was used to pressurise the holes during the spinning and the draw. This was found to be necessary as torsional stresses resulting from spinning greatly distorted the microstructure, leading to hole collapse. This was minimized by applying pressure of up to 80 mBar. The helical core fibres were drawn to diameters of 250 – 300 μm with core off-sets of 80 – 95 μm, hole spacing Λ of 5 μm and hole diameter d of 2.5 μm; this gave a d/Λ of approximately 0.5. The lowest spin pitch was 1.88 mm. The SLB fibres were of similar dimensions with a spin pitch as low as 1.5 mm. Examples of the fibres are shown in Fig. 2.

#113937 - $15.00 USD Received 13 Jul 2009; revised 19 Aug 2009; accepted 19 Aug 2009; published 25 Aug 2009

3. Characterisation

3.1 Helical-core fibres

Circular birefringence places the polarisation modes of the fibre on the poles of the Poincare Sphere. If light with a linear polarisation is launched, its polarisation will remain linear but the plane of polarisation will rotate as it propagates along the fibre. For helical-core fibres the amount of circular birefringence depends on the properties of the helix: the pitch P, the arc length S and the core off-set Q as shown on Fig. 2, which are related by $S = [P^2 + (2\pi Q)^2]^{1/2}$. The plane of polarisation rotates at a rate of $2\pi(S-P)/SP$ rad/m, giving a beat length of

$$L_B = SP / [2(S - P)] \qquad (2)$$

in the absence of linear birefringence [7,20]. It is noted that the beat length is independent of wavelength. (An analysis including linear birefringence may be found in [9].) A large core offset and small pitch will result in large circular birefringence.

To characterise the fibres, the output of a supercontinuum source (400 – >1750 nm) was linearly polarised using a polarising beamsplitter and launched into the fibre core using a microscope objective lens. The output was imaged onto a camera or spectrometer. The orientation of the output light was determined using an analyser and measurements were repeated for different lengths of each fibre sample, allowing the rotation rate, beat length and therefore circular birefringence to be measured. Figure 3(a) compares the measured beat length to that expected from Eq. (2) and the pitch and core-offset of each fibre. The beat lengths measured ranged from 2.3 to 95 cm, corresponding to spin pitches of 1.88 to 6.3 mm. The experimental and theoretical values typically agreed to within 1%.

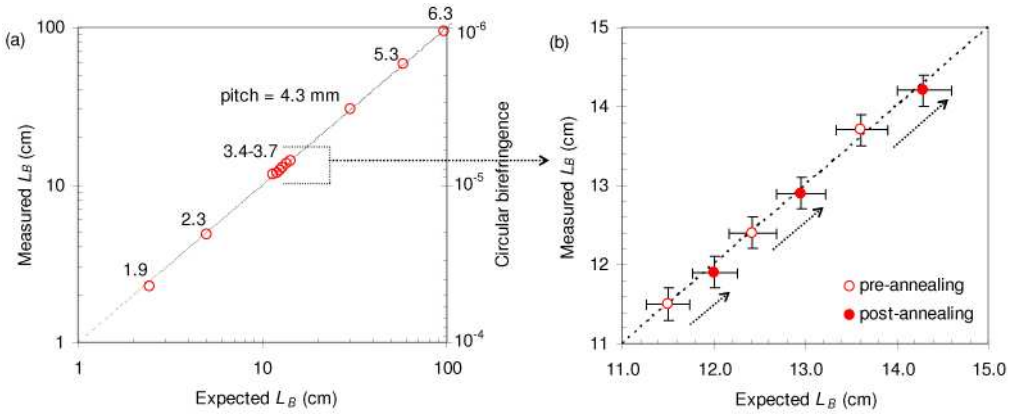

Fig. 3. (a) A comparison of measured and expected beat length as calculated using Eq. (2), for helical core fibres with spin pitch as indicated. The circular birefringence shown was calculated for a wavelength of 1 µm. (b) The same comparison for three fibres before and after annealing. The error bars are indicative of errors arising from experimental measurements of the beat length, pitch and core offset, the latter two becoming increasingly important for small pitch.

One consideration is the effect of spinning on the polymer itself. It is known that the tension used during the fibre draw is stored in the fibre through the alignment of the polymer chains along the fibre axis. Similarly, the torsional stresses created by spinning will be stored through chain orientation, and thus may affect the birefringence properties of the fibres, for example by inducing an additional circular birefringence component through the elasto-optic effect [21]. To investigate this, several of the fibres characterised were annealed for 24 hours at 90 °C to relieve stresses, after which the characterisation was repeated. The beat length was found to be longer after annealing as shown in Fig. 3(b). The torsional stresses were relieved, resulting in the fibre un-twisting to some extent. This caused a slight increase in fibre diameter (and core offset) and an increase in pitch. Using these new parameters the expected

#113937 - $15.00 USD Received 13 Jul 2009; revised 19 Aug 2009; accepted 19 Aug 2009; published 25 Aug 2009

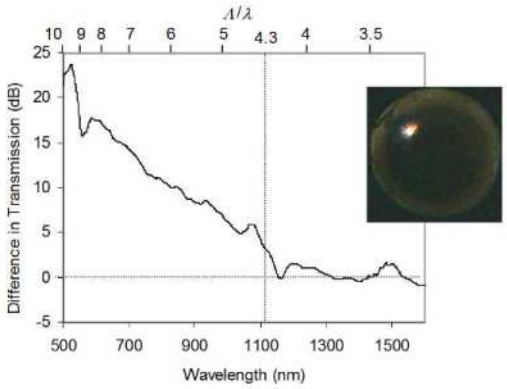

Fig. 4. Difference in transmission between a 13 and a 1.88 mm pitch fibre. The smaller pitch fibre shows higher loss at short wavelengths, resulting from bend loss. The bend loss is expected to affect short wavelengths ($\Lambda/\lambda > 4.3$) for which the *NA* decreases. Inset shows near field of output of a 1.88 mm pitch fibre (10 cm length), showing the transmitted light is red, whilst the light lost due to bend loss is trapped in high order cladding modes. The small oscillations observed in the figure arise from noise in the measurements.

beat length of the fibres was re-calculated and found to once again agree with the measured value. Thus the change in beat length with annealing is purely a geometric effect. This and the results of Fig. 3(a) confirm that the circular birefringence observed is solely a result of the helical core of these fibres and not stresses, and support the assumption that the linear birefringence of these fibers can be neglected.

As the light follows a curved path along the helix, bending loss becomes a consideration. It was observed that the loss of the fibres increased at short wavelength due to bend loss as the spin-pitch was decreased. A comparison of transmission for two fibres with pitches of 13 and 1.88 mm is shown in Fig. 4. For microstructured fibres such as these with a hexagonal hole pattern, the numerical aperture *NA* is known to decrease at short wavelengths [22], owing to an increase in the average index of the microstructured cladding, which arises from an increasing concentration of light in the solid regions of the microstructure. This *NA* decrease makes the fibres more susceptible to bend loss at short wavelengths. Previous work [22] has shown that for fibres with similar d/Λ to that used here, the *NA* begins to decrease at wavelength for which $\Lambda/\lambda > 4.3$. Thus, for the fibres in this work, higher bend loss is expected for $\lambda < 1120$ nm, in good agreement with the experimental results of Fig. 4. Examining the near field of the output with a CCD camera for a high bend loss case (small pitch) indicated that the escaped light was trapped by the cladding in a ring of high order cladding modes.

3.2 Spun linearly-birefringent fibres

In the case of SLB fibres, the beatlength and ellipticity can be described using the Poincare Sphere and simple trigonometric arguments. Figure 1(c) shows the elliptical polarisation which are preserved in the local coordinate system (i.e. a coordinate system that rotates with the core along the fibre). The magnitude of the local linear birefringence vector $\boldsymbol{\eta}$ gives the strength of the linear birefringence the fibre would have if it was not spun and $\boldsymbol{\tau}$ represents the circular birefringence induced by spinning. The vector $\boldsymbol{\rho}$ is the resulting elliptical birefringence vector, and its magnitude gives the strength of the elliptical birefringence. Each type of birefringence is associated with a respective beat length through Eq. (1),

$$\eta = 2\pi / L_p, \tag{3}$$

$$\tau = 4\pi / P, \tag{4}$$

$$\rho = 2\pi / L_B, \tag{5}$$

#113937 - $15.00 USD Received 13 Jul 2009; revised 19 Aug 2009; accepted 19 Aug 2009; published 25 Aug 2009

where L_P denotes the beat length of the unspun fibre owing to the linear birefringence alone, and the additional factor of 2 in Eq. (4) is due to a 2π rotation of the fibre cross-section in the laboratory frame being equivalent to a 4π rotation on the Poincare Sphere [14].

The three types of birefringence are related to one another in the local frame through the simple geometry depicted in Fig. 1(c), which with Eqs. (3) – (5) gives the elliptical beat length and ellipticity ε:

$$L_B = PL_P / \sqrt{P^2 + 4L_P^2}, \tag{6}$$

$$\varepsilon = \tan(\theta / 2) = \tan[\tan^{-1}(2L_P / P) / 2]. \tag{7}$$

Equation (1) then gives the elliptical birefringence. The results of the local frame can be translated into the laboratory frame (i.e. not rotating with the core) using $1/L_B - 1/L'_B = 2/P$, which represents the shift between the two frames, and gives the beat length in the laboratory frame L'_B [13]

$$L'_B = PL_P / \left(\sqrt{P^2 + 4L_P^2} - 2L_P\right). \tag{8}$$

The relationship between these parameters is shown in Fig. 5. In the local frame, spinning the fibre serves to increase the total birefringence and for a fixed L_P a small pitch reduces the elliptical beat length and increases the ellipticity. In the laboratory frame a small pitch similarly increases ellipticity but it decreases the elliptical beatlength, eventually reducing the overall birefringence. It is noted that the elliptical beat length would be affected by the wavelength dependence of the linear beat length L_P.

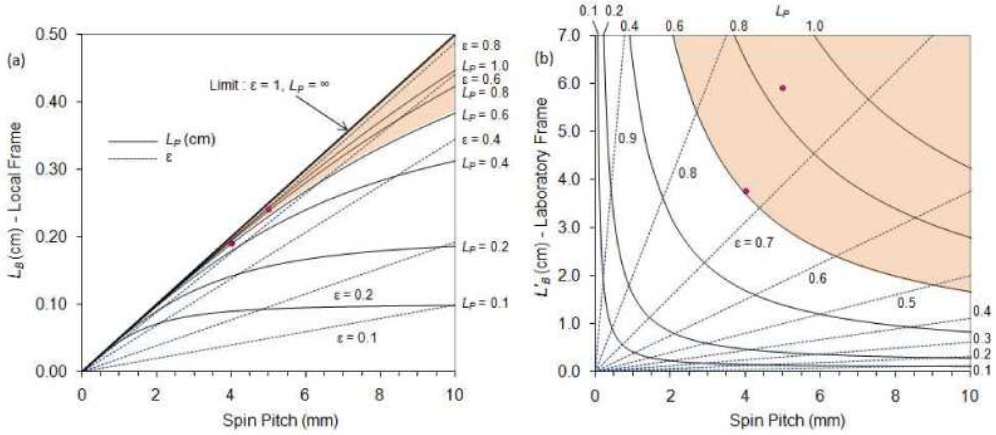

Fig. 5. Ellipticity and beat length for a SLB fibre in (a) the local frame and (b) the laboratory frame. The shaded areas represent the parameter space covered by the fabricated fibres, whilst the data points show the results of specific measurements. Given the wavelength dependence of linear birefringence, the lower L_P values correspond to longer wavelengths.

The SLB fibres were characterised by first measuring the linear birefringence of an unspun fibre, to determine L_P. This was achieved by orienting the input polariser at 45° to the polarisation axes of the core so as to launch an equal amount of light into each linearly polarised mode. The analyser was oriented the same way, creating a fringe pattern in the spectrum. The linear birefringence and beat length were then calculated from the spectrum under the assumption that $B(\lambda) = A\lambda^k$, for constants A and k, and

$$L_B(\lambda) = L\frac{\Delta\lambda}{m\lambda}(k-1)\left[1 - \frac{\Delta\lambda}{\lambda}(k-1)\right]^{-1}, \tag{9}$$

#113937 - $15.00 USD Received 13 Jul 2009; revised 19 Aug 2009; accepted 19 Aug 2009; published 25 Aug 2009

$$B(\lambda) = \frac{m\lambda}{L}\left[\left(1+\frac{\Delta\lambda}{\lambda}\right)^{k-1} - 1\right]^{-1}, \qquad (10)$$

where L is the length of the fibre, $\Delta\lambda$ is the spacing between features in the spectrum and m is the fraction of a fringe those features represent (e.g. 0.5 if $\Delta\lambda$ denotes the spacing between a peak and trough, 1 if $\Delta\lambda$ is from one peak to the next) [5]. The constant k was determined iteratively by estimating its value to find B using Eqs. (9) or (10), and then confirming it with a fit to the derived values of B against wavelength. The birefringence was found to obey $B = 9.6\times10^{12}\lambda^{2.85}$, giving a birefringence and L_P in the range of 1.0×10^{-5} – 2.5×10^{-4} and 5 – 0.6 cm respectively; the wavelength range used was 500 – 1550 nm.

The extent to which a polariser transmits light is related to the distance on the Poincare Sphere between the polariser and polarisation state of the light. Referring to Fig. 1(a), orienting the linear polariser at 45° to the polarisation axes places it on the circle representing the possible output polarisation states of light. Wavelengths close to the polariser will be transmitted, whilst wavelengths on the opposite side of the sphere will not. Orienting the polariser along one of the fibre's polarisation axes (i.e. positioning it on one of the polarisation states on the Sphere) places it at an equal distance from all points on the circle, hence light of all wavelengths will be equally transmitted and the fringes in the spectrum disappear. This requires the wavelength dependence of the birefringence and the length of fibre to be sufficiently large so that at a particular point in the fibre the polarisation state of the light (of the wavelength range examined) will have spread completely around the circle many times over (one fringe corresponds to a complete revolution).

Considering the elliptically birefringent fibres, the location of the polarisation modes is off the equator and so cannot be reached by a linear polariser, hence the fringes in the spectrum described above cannot be fully extinguished. To measure the ellipticity of these fibres required the addition of a Soleil-Babinet phase compensator (SBPC) placed between the fibre output and the analyser. The SBPC is a variable wave plate which allows the phase between the two polarisation states of the fibre to be adjusted, thus allowing the linear polariser to become an elliptical polariser [14] and reach points on the Sphere off the equator.

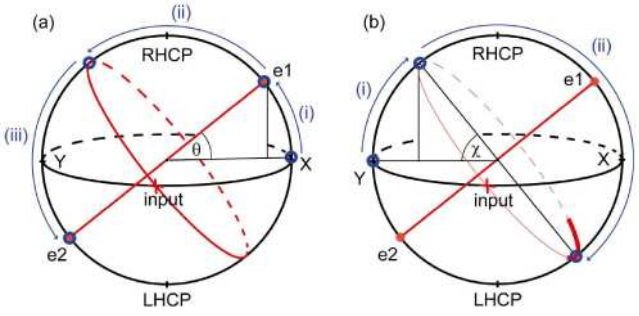

Fig. 6. (a) Measurement of ellipticity using a linear polariser (shown as a blue circle) in combination with a Soleil-Babinet phase compensator, as described in the text, when the light is sufficiently spread over the circle to produce fringes in the spectrum. (b) Alternative measurement for the when the light is not sufficiently spread and occupies only a small arc.

Two approaches were used to characterise the ellipticity. The input polariser remained at 45° to the polarisation axes of the fibre and, with the SBPC initially absent, the analyser was oriented along one of the polarisation axes so as to *minimise* the fringe contrast (note that both polarisers are aligned with respect to the local axes of the fibre). This places the analyser (on the equator) as close as possible to one polarisation mode of the fibre. The SBPC was then added with the fast and slow axis oriented at 45° to the linear polariser. The retardance was increased from zero so as for the fringes to (i) be extinguished, having reached one polarisation mode; (ii) re-appear with maximum contrast, having reached a point on the circle; (iii) re-extinguish, having reached the second polarisation mode. These steps are depicted in

#113937 - $15.00 USD Received 13 Jul 2009; revised 19 Aug 2009; accepted 19 Aug 2009; published 25 Aug 2009

Fig. 6(a). The angle θ, and hence the ellipticity from Eq. (7), can be measured from step (i), whereas steps (ii) and (iii) correspond to changes of $\pi/2$ on the Sphere and were used to calibrate the SBPC [14]. By utilising fringes, this method assumes that light of different wavelengths is distributed completely around the circle.

In the case of a shorter fibre, lower wavelength dependence or narrower wavelength range, the light will not be distributed around the circle but rather occupy an arc, as in Fig. 6(b). Hence, the spectrum cannot produce a series of fringes. Instead, the analyser and SBPC can be positioned on the circle opposite to the light's position, so as to block the light at a single wavelength. The analyser is adjusted to minimise transmission, followed by (i) increasing the retardance until the light is blocked, and (ii) continuing to increase it until transmission in maximized. Step (i) allows the angle χ to be measured, which is complimentary to θ, while step (ii) increases the retardance by π and places the analyser on the same point of the circle as the light.

The above methods were used to characterise a variety of SLB fibres of different pitch and different wavelength (to change the linear birefringence). The pitch and linear birefringence were measured experimentally and used to calculate the elliptical beat length and ellipticity using Eqs. (6) – (8). The ellipticity was also measured experimentally, and in all cases found to be in good agreement with the calculated value. Example values shown in Fig. 5 are L_P = 0.6 cm, P = 4 mm, L_B = 0.19 cm, L'_B = 3.8 cm, ε = 0.71, characterised at 1550 nm, and L_P = 0.85 cm, P = 5 mm, L_B = 0.24 cm, L'_B = 5.9 cm, ε = 0.74, characterised at 1300 nm. The elliptical birefringence was thus of order $5 - 8\times10^{-4}$ in the local frame and an order of magnitude lower in the laboratory frame. As expected, for fixed spin pitches, the ellipticity was observed to increase at short wavelengths owing to a lower linear birefringence component and larger L_P.

4. Conclusion

Spun microstructured fibres using helical-core and SLB fibre geometries have been investigated and a range of polarisation properties realised. Larger circular birefringence, with larger birefringence being typically desirable, can be achieved using identical methods to those employed but utilising a larger core off-set. This would be preferred over a smaller pitch given the hoe distortion that occurs at higher spin rates. A larger air-fraction in the cladding would be required in such cases to minimise the effects of bend loss. Although increasing the air-fraction will usually result in the fibre becoming multimode, the loss experienced by the higher order modes will be greater than for the fundamental mode (e.g. from bend loss) and hence the fibre can still operate in a single-mode fashion if a sufficient length of fibre is used. The fibres used in this work for example with a d/Λ of approximately 0.5 should not be strictly single-mode, however, the presence of higher order modes was not detected in any of the experiments.

Acknowledgements

The authors thank Sergio Leon-Saval for useful discussions and Richard Lwin for assistance with fibre fabrication. This work was performed in part at the Optofab node of the Australian National Fabrication Facility (ANFF) using Commonwealth and NSW State Government funding. ANFF was established under the National Collaborative Research Infrastructure Strategy to provide nano and microfabrication facilities for Australia's researchers.

#113937 - $15.00 USD Received 13 Jul 2009; revised 19 Aug 2009; accepted 19 Aug 2009; published 25 Aug 2009